

Document Details

Document Save Date: 2022-11-07

SGRE guide to producing and interpreting Network Frequency Perturbation (NFP) plots. Other plots in the NFP family

Project name: Grid Forming

Dept.:

Resp. dev.: Andrew J Roscoe

Creation date: 2021/11/22

Revision date: 2022/11/07

Revision: 1

Approved (date):

Initials: AJR

Document History

Rev Number	Revision Date	Author	Changes
0	2021/11/22	AJR	Document created
1	2022/11/07	AJR	Section 3.2. Additional commentary on upstream impedance and #devices operating. Section 4.2. Additional commentary on grid stiffness effects when performing on-site tests by disturbing the “virtual rotor”.

Contents

1	Introduction.....	5
1.1	The “family” of four network-stimulated response plots, of which NFP is one.	5
2	The Network Frequency Perturbation (NFP) plot.....	6
2.1	NFP plot : context	6
2.2	NFP plot : details	6
2.3	NFP plot : example	8
2.4	NFP plot : asymptotes.....	10
2.4.1	NFP plot : asymptotes : droop response asymptote	10
2.4.2	NFP plot : asymptotes : inertia asymptote.....	11
2.4.3	NFP plot : asymptotes : zero-damping phase-step response asymptote.....	11
2.4.4	NFP plot : asymptotes : intercept of inertia and zero-damping phase-step asymptote on NFP amplitude plot at the natural frequency.....	12
2.4.5	NFP plot : asymptotes : estimation of damping coefficient ζ from the NFP plot.....	13
2.5	NFP plot : overlay mask lines	13
3	Simple Generic(V)SM model example	15
3.1	Simple Generic(V)SM model example : analysis.....	15
3.2	Simple Generic(V)SM model example : Network Frequency Perturbation (NFP) plot	17
3.2.1	Simple Generic(V)SM model example : Network Frequency Perturbation (NFP) plot : point of maximum amplitude.....	19
3.2.2	Simple Generic(V)SM model example : Network Frequency Perturbation (NFP) plot : estimation of damping coefficient ζ from the NFP plot.....	20
3.3	Simple Generic(V)SM model example : Power output response to a reference command change	21
4	Practical considerations.....	22
4.1	Practical considerations : time domain considerations and test waveforms	22
4.1.1	Practical considerations : frequency spectra of grid voltages during an NFP plot	22
4.2	Practical considerations : carrying out response sweeps for NFP and NVP plots in simulation and real-world environments.....	23
4.2.1	Practical considerations : NFP sweeps in practice.....	24
4.2.1.1	The NFPxQ plot.....	25
4.2.2	Practical considerations : NVP sweeps in practice	25
4.2.2.1	The NVP plot.....	26
4.2.2.2	The NVPxP plot.....	26
5	Reverse engineering an NFP plot to determine (V)SM parameters	27
5.1	Deducing VSM parameters H , ζ , etc. from the NFP plot.....	27
5.1.1	Basic estimation of droop response from the NFP plot	27
5.1.2	Basic estimation of H from the NFP plot inertia asymptote	27
5.1.3	Basic estimation of total bridge-grid impedance $X + XG$	27
5.1.4	Basic estimation of ζ : How to determine $RNFP_{max}$ and $\omega_n = 2\pi \cdot fn$	28
5.1.5	Estimation of all parameters from NFP plot using multi-parameter fit	28
Appendix A	Derivation of time-domain response of (V)SM rotor	30

References

- [1] A. J. Roscoe, S. J. Finney, and G. M. Burt, "Tradeoffs between AC power quality and DC bus ripple for 3-phase 3-wire inverter-connected devices within microgrids," *IEEE Trans. Power Electron.*, vol. 26, no. 3, pp. 674–688, 2011.
- [2] M. Yu *et al.*, "Instantaneous Penetration Level Limits of Non-Synchronous Devices in the British Power System," *IET Renew. Power Gener.*, vol. 11, no. 8, pp. 1211–1217, 2016, doi: 10.1049/iet-rpg.2016.0352.
- [3] A. J. Roscoe and T. Knueppel, "GC0137 20200430 SGRE Response to VSG_Grid_Code_Draft_Specification_V6_AJ010420 R1. [Annex 11 in GC0137 2021 Consultation]," 2020. [Online]. Available: <https://www.nationalgrideso.com/industry-information/codes/grid-code-old/modifications/gc0137-minimum-specification-required>.
- [4] A. J. Roscoe *et al.*, "Response of a Grid Forming Wind Farm to System Events, and the Impact of External and Internal damping," *IET J. Renew. Power Gener.*, vol. 14, no. 19, pp. 3908–3917, 2021, doi: 10.1049/iet-rpg.2020.0638.
- [5] A. Roscoe *et al.*, "A VSM (Virtual Synchronous Machine) Convertor Control Model Suitable for RMS Studies for Resolving System Operator / Owner Challenges," *15th Wind Integration Workshop*. Vienna, 2016.

Glossary

AC	Alternating Current
CHIL	Controller Hardware-In-the-Loop
DC	Direct Current
DFT	Discrete Fourier Transform
E_{abc}	Voltages at the (virtual) rotor of the (V)SM
GF	Grid Forming
NFP	Network Frequency Perturbation Plot
PHIL	Power Hardware-In-the-Loop
PLL	Phase Locked Loop
PWM	Pulse Width Modulation
ROCOF	Rate of Change of Frequency
RSCAD	RTDS model-creation and execution development environment
RTDS	Real-Time Digital Simulator
SCR	Short Circuit Ratio
SGRE	Siemens Gamesa Renewable Energy
V_{abc}	Voltages at distant upstream “infinite bus”
VSM	Virtual Synchronous Machine

See also Table 3-1.

1 Introduction

This document describes the production and interpretation of, principally, the Network Frequency Perturbation (NFP) plot. The NFP plot indicates the closed loop transfer function of the device, to a specific type of excitation, applied at the distant grid “infinite bus”. The NFP plot graphically shows the amplitude and phase of the active-power response of a device within an AC power network, when the distant upstream “infinite bus” voltage waveforms are frequency-modulated with sub-harmonic frequencies, from 0 Hz to the fundamental.

A frequency modulation of the distant grid voltages is also equivalent to, and can be thought of, a phase modulation.

The NFP plot therefore shows how the active-power output of a device responds to an upstream voltage frequency/phase modulation. By sweeping the frequency of the frequency/phase modulation from zero towards the fundamental AC frequency, it is possible to build up the NFP plot.

The NFP plot shows both the amplitude and phase of the active power response, for the applied amplitude and phase of the to frequency/phase modulated grid voltage waveforms. Therefore the NFP plot can show peaks (i.e. resonances) and troughs of the amplitude of the response, and also whether the active-power response is in-phase or out-of-phase with the distant grid voltage perturbation. Several properties of a Grid Forming (GF) device can be identified and quantified by examining, or reverse engineering, the NFP plot for a device:

- The lowest modulation frequencies allow the frequency/power droop response to be evaluated/estimated.
- The low-mid range modulation frequencies allow rolloff of droop response to be evaluated, i.e. if the primary response power is bandwidth-limited, for example due to the use of a steam or gas turbine with a slow response.
- The mid-range modulation frequencies allow the inertia and damping response to be evaluated, along with any rotor resonance effects
- The upper frequencies allow the response of the device to grid phase steps, via the total impedance between the (virtual) rotor and the distant upstream grid (“infinite bus”), to be evaluated.
- “Odd” behaviour at the upper frequencies, i.e. phase wrapping, can also be used as a tool to identify non Grid Forming (GF) devices, that do not provide the same responses to grid phase steps, and can provide responses that are 180° to those that a GF device might provide.

The NFP plot was initially developed during ~2011-2012, and applied to the work described in the paper [1]. This was to support an industrial project. The NFP plot was used to tune the performance of a GF Virtual Synchronous Machine (VSM) (called “Voltage Drive Mode” in [1]), coupled to a DC bus with stored energy available, such that it matched the dynamic performance of a turbo-diesel powered Synchronous Machine (SM), in terms of droop and prime mover response, inertia, and damping. [Interestingly, the GF VSM developed in [1] contains a PLL, but is grid forming, due to the way the control loops and PLL are configured. “Use of a PLL” does not necessarily mean that a device is non-GF!]. The NFP plot was first introduced in literature in the paper [2], when it was used to compare the performance of Grid Forming (GF) and non-grid-forming devices.

The NFP plot was then further introduced in the National Grid workgroup GC0137 document from SGRE [3].

1.1 The “family” of four network-stimulated response plots, of which NFP is one.

The Network Frequency Perturbation (NFP) plot is the most important of a family of 4 plots [3]. This document focusses on the production and interpretation of the NFP plot. However, the other three plots in the “family” may be useful in future, although they have not been explored yet, to the author’s knowledge:

- 1) NFP plot showing **active power** responses to grid **frequency/phase modulations**
- 2) NFPxQ plot showing cross-linkage of **reactive power** responses to grid **frequency/phase modulations**

and

- 3) NVP (Network Voltage Perturbation) plot showing **reactive power** responses to grid **voltage modulations**
- 4) NVPxP plot showing cross-linkage of **active power** responses to grid **voltage modulations**

The “other three” plots are briefly discussed in sections 4.2.1.1, 4.2.2.1 and 4.2.2.2.

2 The Network Frequency Perturbation (NFP) plot

The NFP plot [2][3] relates a grid frequency/phase perturbation to an active power response at the device terminals. There are 3 other plots in the family of responses (see section 1.1, and [3]), but the NFP plot is considered to be the most important.

2.1 NFP plot : context

Figure 2-1 shows the context of a SM or VSM embedded within the power system. In this analysis, the SM rotor or VSM bridge is separated from the stator (or virtual stator) by a pu reactance X . This is the pu transient reactance X'_d in a SM, or the primary filter reactance in a VSM. However, the total impedance to the grid also includes other upstream elements including transformers and transmission lines. In this analysis, only the dominant inductive series elements are considered, and both (V)SM induced rotor and grid voltage magnitudes are considered to be nominal at 1pu. Angle δ_{RS} describes the angle between the (virtual) rotor and the (virtual) stator, while δ_{RG} describes the angle between the (virtual) rotor and the distant upstream grid. Figure 2-1 also shows a parallel current and power path via a squirrel-cage icon. This represents, in a real SM, the damper windings which introduce an additional real power flow that is proportional to the slip frequency between ϕ_R and ϕ_S .

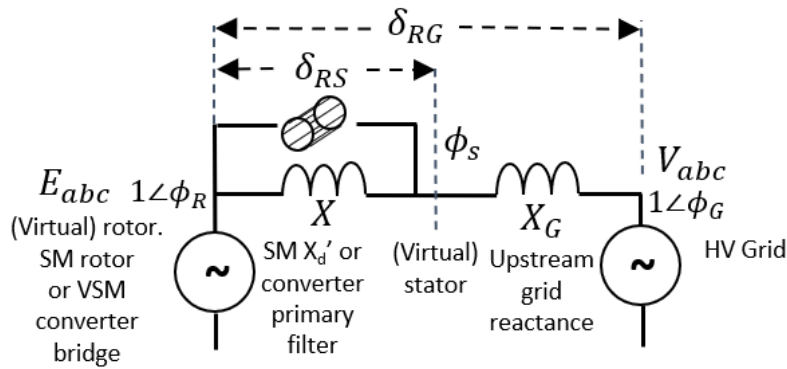


Figure 2-1 : Context for SM or VSM embedded within power system

2.2 NFP plot : details

To generate the NFP plot the real or simulated device is placed within a hypothetical or ‘test’ (e.g. “Power Hardware in-the-Loop” PHIL or “Controller Hardware in-the-Loop” CHIL) power system, such as Figure 2-1, in which the grid frequency is forced and modulated in a sinusoidal fashion, centered on the nominal frequency f_0 , with a small frequency deviation, amplitude Δf applied at frequency f_{NFPmod} . This can be expressed as:

$$f(t) = f_0 + \Delta f \cos(2\pi f_{NFPmod} t + \phi_{\Delta f}) \quad (2-1)$$

The value of f_{NFPmod} is swept across a broad range, from $\sim 10^{-3}$ Hz to ~ 20 Hz or optionally up to ~ 50 Hz or ~ 60 Hz, whatever the fundamental frequency of the AC network is. The arbitrary angle $\phi_{\Delta f}$ represents a “random” steady-state angle offset, which should remain constant.

The frequency modulation given by (2-1) can also be expressed, and thought of, as a phase modulation. This is demonstrated and quantified in section 4.1.

The device responds to this changing frequency/phase with a modulated active power output:

$$P_{set} + \Delta P \cos(2\pi f_{NFPmod} t + \phi_{\Delta P}) \quad (2-2)$$

The amplitude of the frequency modulation Δf is kept small enough that no unnatural saturation of device control loops occur.

- Inertia power saturation limit: if the suspected device inertia is H s, then to keep peak output power modulation amplitude below ΔP_{max} pu (i.e. 0.25 pu), accounting for the approximate expected power output $\Delta P = -2H (df/dt)/f_0$ and the differentiation of frequency to df/dt
- Droop response limit: if the suspected device droop slope (pu frequency drop for 1 pu active power output) is D_f , then $\Delta f < \Delta P_{max} D_f f_0$

$$\Delta f < \frac{\Delta P_{max}}{2H} \frac{f_0}{2\pi f_{NFP_{mod}}} \text{ Hz (Inertial limit)} \quad (\text{whichever is smaller}) \quad (2-3)$$

$$\Delta f < \Delta P_{max} D_f f_0 \text{ Hz (Droop limit)}$$

This would, for example, limit Δf to ~ 0.5 Hz at low values of modulation frequency, dropping to ~ 0.01 Hz at a 10 Hz modulation frequency for an $H = 8$ device.

ΔP and $\phi_{\Delta P}$ can be found either by:

- Placement of the actual or simulated device and its transformer impedance(s), including its control system, within a real or simulated test environment (Figure 2-1), and carrying out the modulated sweep described above. In this case, it is important to perform Fourier analysis of both the generated frequency deviation and measured power outputs using coherent sample sets of the frequency (2-1) used to generate the waveform, and the measured power. The same window lengths and parameters must be used for the pair of Fourier analyses so that not only the magnitude of ΔP is correctly determined, but also its phase $\phi_{\Delta P}$ which must be determined accurately, relative to the phase of the frequency modulation cosine waveform defined by (2-1).
- It is possible to obtain the NFP plot on-site, for a large-scale multi-MW device and without a test environment. The modulating frequency sweep can be injected as small open-loop adjustments to real-time PWM patterns (voltage angles). Fourier analyses of the frequency offsets applied at the bridge, and the power output, can reveal the NFP plot, on the assumption that the distant upstream grid phase/frequency is relatively steady throughout the test. Essentially the perturbations are applied at the rotor, while the grid frequency/phase deviations remain at zero, compared to the opposite scenario of Figure 2-1. There is a risk of locally elevated levels of flicker and voltage (inter)harmonics during the test period, if the device has a high power rating compared to the local grid stiffness.
- It might also be possible to reverse engineer the NFP plot from natural variations of grid phase/frequency over a long test period, if the test period contains suitable grid frequency/phase events to allow the responses to be determined above the background noise. No method to practically achieve this is claimed nor presented in this report.
- Classical analysis of the device transfer functions. For instance, the (V)SM equations (3-11) & (3-12) describe the NFP plot shape for a Generic VSM_{Int} (3-12) described with a simple model. These only consider the simplest power-to-angle control loop, and do not account for additional control loops and interactions with voltage magnitude controls. Therefore, for a real device with a complex control system, potentially incorporating Park and Clarke transformations, more advanced state-space models may be required to reveal a truly accurate NFP plot, that accounts for all interacting control loops and linearisations.

In all cases, the amplitudes of the voltages are kept (or assumed to remain) constant at 1 pu, so that the analysis is purely an examination of the interaction between active power and frequency/phase at the grid.

The NFP response calculation requires:

- The stimulus amplitude Δf from the Fourier analysis of the stimulus
- The response amplitude ΔP (where ΔP is in per-unit (pu) from the Fourier analysis of the response
- The stimulus phase $\phi_{\Delta f}$ from the Fourier analysis of the stimulus
- The response phase $\phi_{\Delta P}$ from the Fourier analysis of the response.

$$R_{NFP} = \frac{\Delta P \angle \phi_{\Delta P}}{\left(\frac{\Delta f \angle \phi_{\Delta f}}{f_0} \right)} \quad (2-4)$$

Essentially, the NFP plot of R_{NFP} (2-4) shows the amplitude of the power response of the device, in pu, to a cosinusoidally modulated grid frequency, with the frequency of the modulation swept and plotted as the x axis. The grid frequency modulation amplitudes Δf must in practice be small compared with f_0 , and the results are normalised by (2-4) to a pu modulation amplitude $\Delta f / f_0$ to ensure consistency of plotting.

The NFP amplitude plot shows $|R_{NFP}|$ on the y axis against modulation frequency $f_{NFP_{mod}}$ (Hz) on the x axis. The plot is best made by plotting both axes using logarithmic scales. The y axis can either be interpreted as:

- the amplitude of the sinusoidally varying power response of the device, in pu, to a 1 pu amplitude sinusoidal grid frequency variation at $f_{NFP_{mod}}$
- OR, (with the same values on the x and y axes, and conceptually slightly more meaningful), **the amplitude of the sinusoidally varying power response of the device, in % pu, to a 1 % pu amplitude sinusoidal grid frequency variation at $f_{NFP_{mod}}$** . This second format essentially applies a x100 scaling to both numerator and denominator of (2-4), which cancel out.

The NFP phase plot shows $\angle R_{NFP}$, in degrees on the y axis, against modulation frequency $f_{NFP_{mod}}$ (Hz) on the x axis. The plot is made by plotting the x axis using the same logarithmic scale as the amplitude plot, but with a linear y scale. The y axis is best ranged from -90° to +27°, with +90° in the middle of the plotted y range.

2.3 NFP plot : example

As a visual example, Figure 2-2 and Figure 2-3 show the NFP plot, plus reverse-engineered overlays and asymptotes, for a GF VSM.

- The GF VSM has internal damping [4], and a damping coefficient of $\zeta=1$ in the considered grid scenario. In those respects, it is different to a conventional SM, which has external damping [4], and normally has a damping coefficient ζ that is significantly less than 1.
- However, in other respects the example VSM has been configured to behave very like a real SM, with $H = 4$ s, coupled to a prime mover, operating on a 4 % frequency (to 1 pu power) droop slope, with the prime mover having a response with a time constant $\tau_P=1$ s. This would provide a response similar to that of a SM coupled to a turbo-diesel genset, for example.

The magnitude and phase plots, Figure 2-2 and Figure 2-3, show a number of typical and useful features that will be described throughout the rest of this guide.

Network Frequency Perturbation (NFP) plot : Magnitude :
 $f_0 = 50 \text{ Hz}$, $\tau_\delta = 2 \text{ ms}$

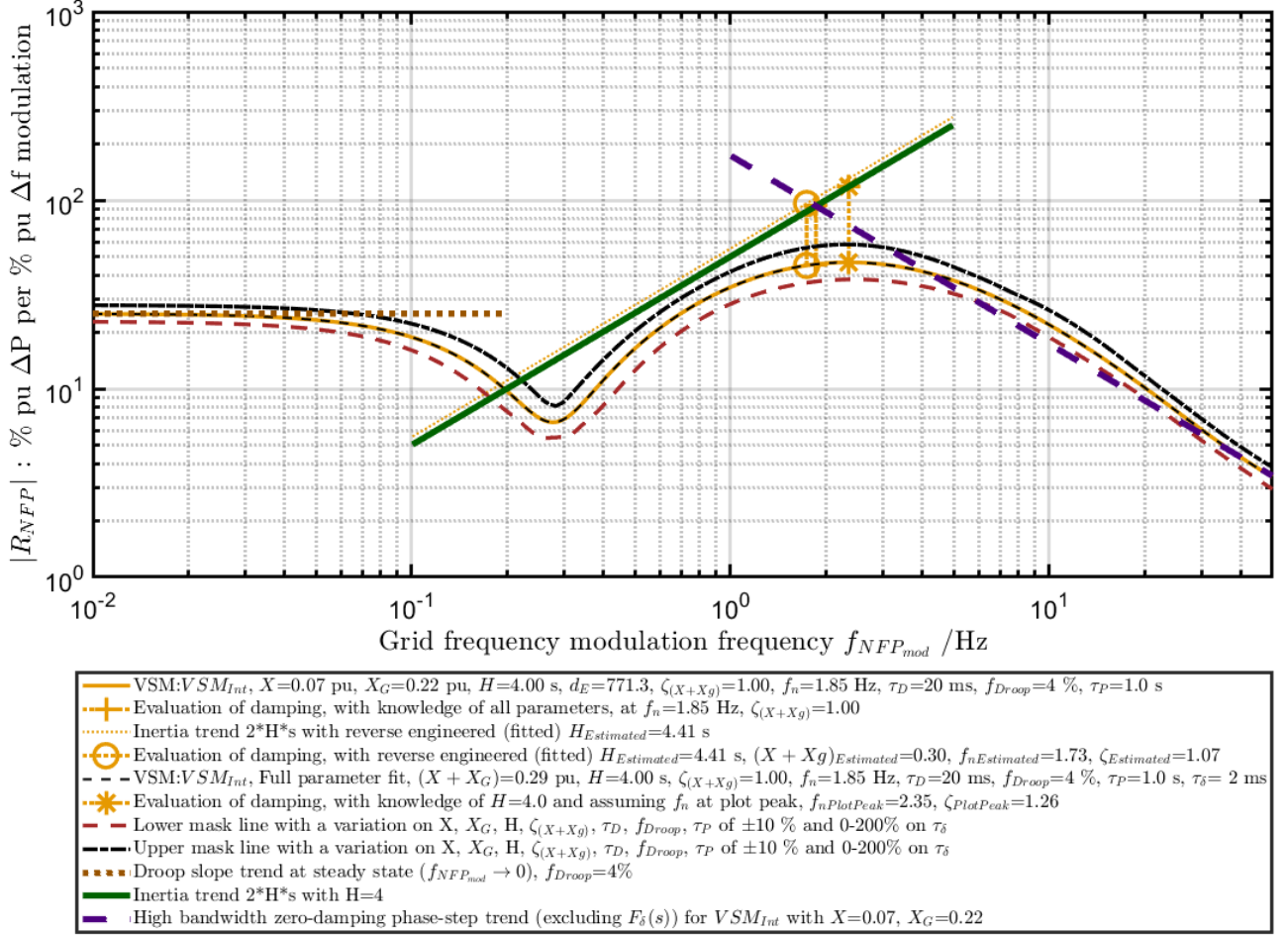


Figure 2-2 : Example NFP plot (magnitude), with reverse engineering overlay, for a VSM configured to operate similarly to a real SM with inertia $H=4\text{s}$, damping coefficient $\zeta=1$, coupled to a prime mover with a response time constant $\tau_p=1\text{s}$.

Network Frequency Perturbation (NFP) plot : Phase :
 $f_0 = 50 \text{ Hz}$, $\tau_\delta = 2 \text{ ms}$

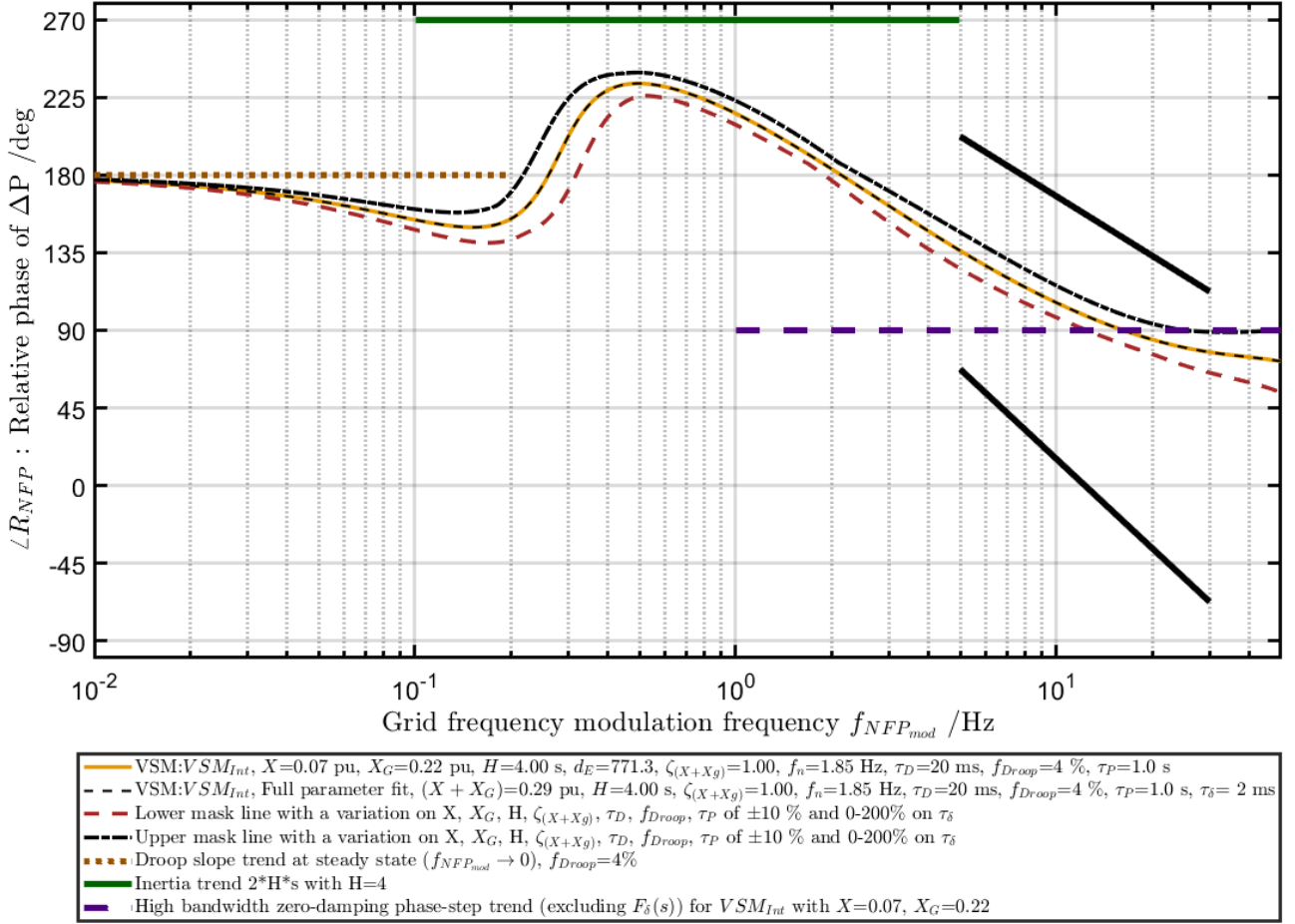


Figure 2-3 : Example NFP plot (phase), with reverse engineering overlay, for a VSM configured to operate similarly to a real SM with inertia $H=4\text{s}$, damping coefficient $\zeta=1$, coupled to a prime mover with a response time constant $\tau_P=1\text{s}$.

2.4 NFP plot : asymptotes

There are 3 important asymptotes on the NFP plot, plus a general rule concerning the right-hand side of the plot. Some of the mathematical derivation of these asymptotes requires use of a Generic VSM model, which is described later in section 3. However, in terms of generally describing the NFP plot, introducing the asymptotes first may suit many readers. Optionally, reading section 3 before reading the remainder of section 2 may suit some readers.

2.4.1 NFP plot : asymptotes : droop response asymptote

In the most basic case, with a steady-state frequency deviation of $\Delta f \text{ Hz}$, at a zero or very low value of modulated frequency $f_{NFP_{mod}}$, the expected power output will be $\Delta P = (\Delta f / f_0) / D_f$ and $\phi_{\Delta P} = \pi$ (i.e. 180°) as the device responds on a droop slope of $D_f \text{ pu frequency to 1 pu power}$. The 180° is important here since as frequency goes down, power output should increase. In this basic case, only the drooped response is acting, and all other mechanisms are inactive since the modulation frequency is so low and there are no transient events occurring, just a steady-state frequency offset. Therefore by (2-4):

$$R_{NFP} = -1/D_f \quad (2-5)$$

This defines an asymptote on the left-hand side of the NFP plot. For every device providing a drooped power response to frequency, the NFP plot should merge with this asymptote which is a horizontal line intercepting:

- $|R_{NFP}| = 1/D_f$ on the y axis ($f_{NFP_{mod}} \rightarrow 0$) of the amplitude plot
- $\angle R_{NFP} = 180^\circ$ on the y axis ($f_{NFP_{mod}} \rightarrow 0$) of the phase plot

The droop asymptote is shown on Figure 2-2 and Figure 2-3 as a horizontal brown dotted trace, towards the left hand side.

For a traditional SM coupled to a mechanical prime mover and governor system, the droop response has a finite response time and phase lag. Therefore, for all these traditional generators, the amplitude of the droop response $|R_{NFP}|$ is expected to fall below $1/D_f$ as $f_{NFP_{mod}}$ rises above 0 Hz and the prime mover response become “cut off”. Likewise it is expected that the phase of the response $\angle R_{NFP}$ will increasingly lag behind 180° as $f_{NFP_{mod}}$ rises above 0 Hz.

2.4.2 NFP plot : asymptotes : inertia asymptote

The second key asymptote is that of inertial response. This is defined using the simplistic approximation equation linking electrical frequency and the expected power output during a constant-ROCOF event. It should be remembered that this equation ignores all the effects of rotor resonance and damping, and can only be truly accurate during established and linear frequency ramps with a completely constant ROCOF.

$$\Delta P = -\left(\frac{2H}{f_0}\right) \frac{df}{dt} \quad (2-6)$$

Accounting for the frequency modulation $f_{NFP_{mod}}$ applied during the NFP process (2-1) and the differentiation of frequency in (2-6), the predicted asymptote will be:

$$\Delta P = -\left(\frac{2H}{f_0}\right) \Delta f 2\pi f_{NFP_{mod}} \cdot -\sin(2\pi f_{NFP_{mod}} t) = \left(\frac{2H}{f_0}\right) \Delta f 2\pi f_{NFP_{mod}} \sin(2\pi f_{NFP_{mod}} t) \quad (2-7)$$

This has a phase which is only 90° behind the cosine waveform of (2-1), i.e. 90° advanced compared to the 180° phase of $|R_{NFP}|$ for a droop response (section 2.4.1), and a peak amplitude of $\left(\frac{2H}{f_0}\right) \Delta f 2\pi f_{NFP_{mod}}$.

This leads via (2-4) to another straight line asymptote on the NFP plot (both amplitude and phase plots):

$$R_{NFP} = 2H \cdot 2\pi f_{NFP_{mod}} \angle 270^\circ \quad (2-8)$$

- $|R_{NFP}| = 2H \cdot 2\pi f_{NFP_{mod}}$ on the y axis of the amplitude plot, which crosses the plot diagonally from bottom-left to top-right.
- $\angle R_{NFP} = 270^\circ$ on the y axis of the phase plot, i.e. 90° advanced compared to the 180° phase of the $|R_{NFP}|$ asymptote for a droop response (section 2.4.1).

The inertia asymptote is shown on Figure 2-2 and Figure 2-3 as a thick solid green line.

The inertia asymptote line defines an idealistic response expected from a generator during a sustained constant-ROCOF frequency ramp. It ignores the effects of droop response, rotor resonance, and damping. Every device that is claiming to implement an inertial response should provide a response which approaches this line, both in amplitude and phase, over a range of modulation frequencies $f_{NFP_{mod}}$ at which the rotor response is dominant over drooped and damping responses. The approach of the phase, i.e. a noticeable shift from the “default” 180° drooped phase response to a more advanced phase towards 270° , is a particularly important criteria for demonstrating dominance of an inertial response over the relevant range of $f_{NFP_{mod}}$ frequencies. It is possible, over the relevant range of $f_{NFP_{mod}}$ frequencies, to provide a boosted magnitude of response $|R_{NFP}|$, but without a clear phase advance relative to a drooped response at 180° . This should be interpreted as an enhanced droop/damping response, not as an inertial response.

Likewise, it is possible for a device to offer both inertia and a fast-responding droop response such that the droop response is still significant at higher $f_{NFP_{mod}}$ where (conventionally) inertia and rotor resonance is dominant. In such a case, the phase may rise above 180° but not reach all the way to 270° . This can indicate a mix of significant inertia PLUS fast-acting drooped/damping response.

2.4.3 NFP plot : asymptotes : zero-damping phase-step response asymptote

The third asymptote is a phase-step response asymptote, which relates to only the most rapid-responding power outputs. This response line, as opposed to the inertia asymptote, has, on the amplitude plot, a negative gradient, i.e.

the power output magnitude decreases with increasing modulation frequency. Also, on the phase plot, $\angle R_{NFP}$ tends to become more lagged with increasing modulation frequency, although, for a GF device, the gradient of $\angle R_{NFP}$ normally flattens as the modulation frequency approaches nominal frequency. The response can be written down by examination of a simple (VSM) model (described later in section 3) as shown in Figure 3-1, to only the highest-frequency components of f_G , which directly cause a power output, as the simplest open-loop path from f_G to P_{VSM} or P_{SM} , without any closed-loop action through the filtering effects of inertia or the $1/s$ terms in the closed loop.

Firstly, from (3-12), the expected response for a VSM with internal damping, or a SM with zero damping:

$$R_{NFP} = \frac{\Delta P_{VSMint}}{f_G} = -\left(\frac{\omega_0}{s}\right)\left(\frac{X}{X + X_G}\right)F_\delta(s)\frac{1}{X} \quad (2-9)$$

If $F_\delta(s)$ is ignored, this simplifies to:

$$R_{NFP} = \frac{\Delta P_{VSMint}}{f_G} \approx -\left(\frac{\omega_0}{s}\right)\left(\frac{1}{(X + X_G)}\right) \quad (2-10)$$

Secondly, from (3-11), the expected response for a SM with external damping:

$$R_{NFP} = \frac{\Delta P_{SM}}{f_G} = -\left(\frac{\omega_0}{s}\right)\left(\frac{X}{X + X_G}\right)F_\delta(s)\left\{\frac{1}{X} + F_S(s)\frac{k_S \cdot s}{\omega_0}\right\} \quad (2-11)$$

Both asymptotes intercept the inertia asymptote.

The first (VSM with internal damping, or a SM with zero damping) expression is easier to analyse, and, if the effect of $F_\delta(s)$ is ignored, becomes a straight-line asymptote that intercepts the inertia asymptote (in amplitude, not phase) near the point of resonance. This turns out to be a really useful asymptote, and can later be used as a tool to reverse-engineer the damping coefficient from an NFP plot. This first expression still has meaning for a SM with finite external damping, since for both VSM and SM it represents the zero-damping phase-step response asymptote.

$$R_{NFP} \approx -\left(\frac{2\pi f_0}{j2\pi f_{NFPmod}}\right)\left(\frac{1}{(X + X_G)}\right) \approx j\left(\frac{f_0}{f_{NFPmod}}\right)\left(\frac{1}{(X + X_G)}\right) \quad (2-12)$$

- $|R_{NFP}| = \left(\frac{f_0}{f_{NFPmod}}\right)\left(\frac{1}{(X + X_G)}\right)$ on the y axis of the amplitude plot, which crosses the plot diagonally from the middle to the bottom-right.
- $\angle R_{NFP} = 90^\circ$ on the y axis of the phase plot, i.e. 90° lags compared to the 180° phase of the $|R_{NFP}|$ asymptote for a droop response (section 2.4.1). It's phase is 180 degrees different to the inertial asymptote.

The “High bandwidth zero-damping phase-step (excluding $F_\delta(s)$)” response asymptote is shown on Figure 2-2 and Figure 2-3 as a thick, dashed, purple line.

2.4.4 NFP plot : asymptotes : intercept of inertia and zero-damping phase-step asymptote on NFP amplitude plot at the natural frequency

While the phases of the inertia and zero-damping phase-step asymptotes are different by 180 degrees, the amplitudes of the zero-damping phase-step asymptote (2-12) and inertia asymptotes (2-8) intercept each other on the amplitude plot at the undamped resonance frequency! This is a handy relationship. It can be shown by equating the magnitude components of the inertia (2-8) and zero-damping phase step (2-12) asymptotes:

$$|R_{NFP}| = \left(\frac{f_0}{f_{NFPmod}}\right)\left(\frac{1}{(X + X_G)}\right) = 2H \cdot 2\pi f_{NFPmod} \quad (2-13)$$

i.e.

$$2\pi f_{NFPmod} = \sqrt{\left(\frac{2\pi f_0}{2H}\right)\left(\frac{1}{(X + X_G)}\right)} = \omega_n \quad (2-14)$$

Hence the intercept of the two asymptotes happens at the undamped resonance frequency where $2\pi f_{NFPmod} = \omega_n$.

It also implies that the magnitude of the asymptotes where this happens can be easily determined from the inertia asymptote slope and the natural frequency:

$$|R_{NFP_InertiaAsymptoteAtUndampedResonanceFrequency}| = 2H \cdot \omega_n = 2H \cdot 2\pi \cdot f_n \quad (2-15)$$

which can also be expressed (by resubstitution of ω_n from (3-4):

$$|R_{NFP_InertiaAsymptoteAtUndampedResonanceFrequency}| = 2H \cdot \sqrt{\frac{\omega_0}{2H(X + X_G)}} = \sqrt{\frac{2H\omega_0}{(X + X_G)}} \quad (2-16)$$

This also implies that, in the absence of any knowledge of a VSM from its parameters, with only access to a graphical NFP plot or the numerical trace of it, one might guess at the natural undamped resonance frequency by fitting/laying straight lines against the NFP plot and estimating their crossing point.

The intercept of the two asymptotes, in magnitude, is shown on Figure 2-2. It can be seen that (roughly) this aligns with the peak of the actual (damped) NFP magnitude plot. It also aligns (exactly in this simple case) with the (in this case known) undamped natural frequency of the example device in its environment, $f_n=1.85$ Hz.

This intercept point also provides another important function. It allows the damping coefficient to be determined. This is described in section 2.4.5

2.4.5 NFP plot : asymptotes : estimation of damping coefficient zeta ζ from the NFP plot

The damping coefficient can be determined from the NFP plot, assuming that the device conforms approximately to the Generic VSM model described in section 3. To explain how this is done, requires the mathematics of section 3, in particular section 3.2.1 and 3.2.2. The overall result is that:

Finally this extremely helpful equation drops out from (3-23):

$$\zeta \approx \frac{|R_{NFP_InertiaAsymptoteAtUndampedResonanceFrequency}|}{2|R_{NFP_max}|} \quad (2-17)$$

This means that the damping coefficient zeta, ζ is related very simply to the ratio between the peak NFP amplitude response and the amplitude at the point at which the inertia and the zero-damping phase-step asymptotes cross. The peak NFP amplitude response and the asymptote crossing should both occur roughly at the undamped resonant frequency at $2\pi f_{NFP_mod} = \omega_n = 2\pi \cdot f_n$. If the zero-damping phase-step asymptote is not available or is unclear, then the inertia asymptote line can be used alone, with its amplitude sampled at the undamped resonant frequency.

2.5 NFP plot : overlay mask lines

In addition to the asymptotes, mask lines can be placed on the NFP plot, against which devices might be assessed for compliance. For example, if a device claims to have certain characteristics that match those of the example device shown in Figure 2-2 and Figure 2-3, then mask lines can be generated that allow certain percentage deviations from each of the key parameters. These can be generated using a Monte-Carlo approach, using the frequency domain model of section 3, analysing all the worst-case combinations of deviations of parameter values.

Examples of these masks are shown on Figure 2-2 and Figure 2-3, with ± 10 % deviations allowed on several parameters, and 0-200 % on τ_δ . Even with 10 % deviations allowed, the mask lines appear relatively tight on Figure 2-2 and Figure 2-3. This suggests that a significant deviation from a “target” NFP plot shape probably represents quite a large deviation in actual parameterisation. The technique therefore ought to be a reasonable way of assessing whether a device is operating with (roughly) the published parameterisation, or not.

Also shown on Figure 2-3, the phase NFP plot, are two thick black lines to the right-hand side of the plot. These are based on typical trajectories of the phase of the NFP plots, for GF devices. The concept is that ALL GF devices ought to provide responses that fit between these lines, whatever the parameterisation. The lines trend towards more negative phases as the modulation frequency approaches fundamental. The lines should also trend towards the zero-damping phase-step inertia asymptote (section 2.4.3), which, in theory, is horizontal on this plot, by (2-12). The exact placement of these phase mask lines is still a matter for further research/discussion, and needs to be corroborated against typical results recorded from real devices, not just theoretical example plots. However, the general principle is

probably sound; that GF devices can be recognised by their distinctive amplitude and phase trajectories over this “upper frequency” region of the NFP plot. The NFP plot phase for a GF device tends to drop towards 0-90°, but then levels off and does not exhibit phase wrapping. This compares with typical NFP plot trajectories for grid-following devices that tend to exhibit phase-wrapping over this “upper frequency” region of the NFP plot [2].

3 Simple Generic(V)SM model example

The context for this model is described in section 2.1 and Figure 2-1.

3.1 Simple Generic(V)SM model example : analysis

This model was originally developed for the GC0137 input [3], and also presented in the IET journal paper [4] which contains distilled information describing the effect of damping, and how a GF device usually provides “internal” (virtual) damping, which is different to the “external” damping that appears as real power at a SM terminals. The “external” damping is due to the induction-machine slip-related power due to damper windings and/or parasitic effects in the SM. In contrast, there is no such natural “slip related” power output in a converter device, so the damping is by default provided “internally” and does correspond to an actual slip-related power exchange. Initial investigations suggest that adding “external” damping to a GF VSM might introduce or require high-frequency dynamics that could be undesirable from both a manufacturer and network perspective. In particular, relationships for a VSM with internal damping were derived and presented in [3] and [4]. These are the basis for the sections which follow, although some improvements have subsequently been made.

Figure 3-1 shows simplest possible linear control diagram that can be drawn that encompasses both a real SM, and a VSM behaviour, in terms of active-power response to upstream grid frequency (and hence phase). This model makes no attempt to account for resistive elements in a network. The assumed relationship is that power flow is proportional to the angle across the inductive reactance of the key components, and that angles are small enough that $\sin(\delta) \approx \delta$.

It must be appreciated that a real GF converter system, particularly one that uses Park/Clarke transforms within the control loops, will potentially require a MUCH more complex control diagram than Figure 3-1 shows, in order to represent it accurately, especially if the response needs to be linearised for analysis. Nevertheless, the simple Generic (V)SM model allows a number of the key expected GF VSM features to be quantified, and produces some important results in the context of the NFP plot.

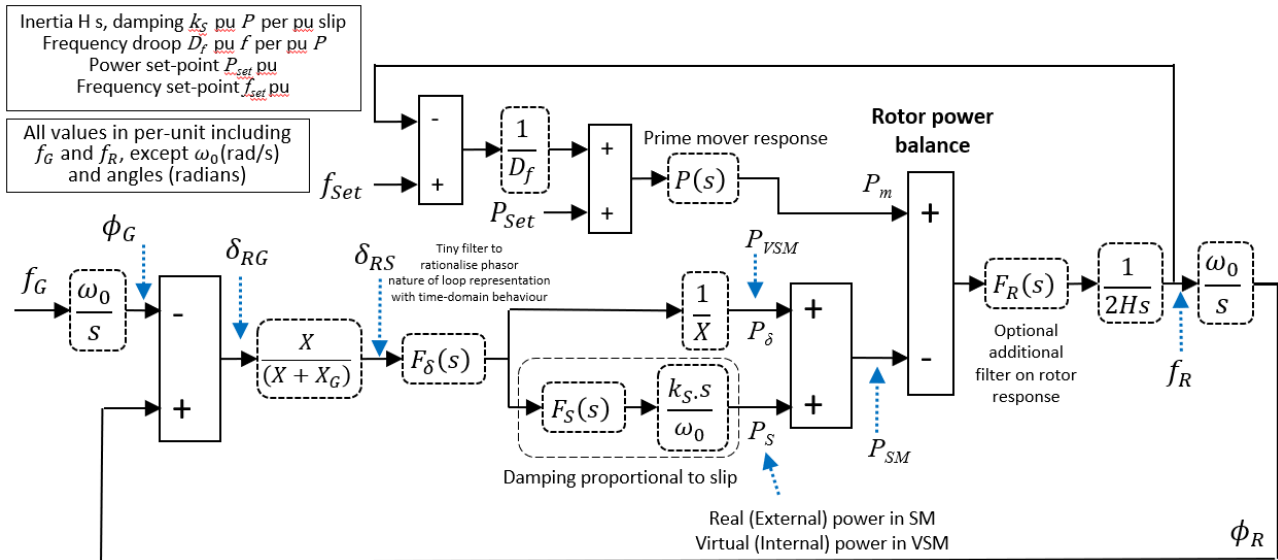


Figure 3-1 : Simplified linearised model of Generic SM or VSM embedded within power system, assuming voltage ~ 1 pu, frequency ~ 1 pu, and $\sin(\delta) \approx \delta$. Adapted from [3] and [5].

D_f	Frequency/power droop slope, pu frequency per pu power
δ_{RG}	Angle between virtual rotor and distant stiff grid
δ_{RS}	Angle (radians) between (virtual) rotor voltage and (virtual) stator terminals in a (V)SM
$F_\delta(s)$	A small-time-constant filter on the perception of δ_{RS} , added to the models of both SM and VSM, but not part of the VSM control software. This tiny filter rationalises the phasor nature of the Figure 3-1 loop representation, with time-domain behaviour of actual 50 Hz waveforms. It may also be used to partly represent the use of Park/Clarke transform algorithmic approaches, although detailed analysis of a GF converter system that uses Park/Clarke transforms requires a significantly more complex frequency-domain model than Figure 3-1 shows.
f_G	Frequency at distant (stiff) grid, in pu
f_{Set}	Frequency setpoint, in pu
$F_R(s)$	An optional filter applied within a VSM control system, which applies additional filtering in series with the rotor inertia dynamics. For example, filter zeros placed at all integer multiples of actual frequency stop the VSM virtual rotor from oscillating at all, during the presence of harmonics and unbalance.
$F_S(s)$	A small-time-constant filter on the evaluation of the damping power P_S , added to both the real VSM control system, and the system model for SM
k_S	Damping power (pu) per pu slip
P_m	(Virtual) mechanical power input to a (V)SM rotor, from a (virtual) prime mover/governor
P_S	Damping power (real/external or virtual/internal) due to the slip of ϕ_R against ϕ_S
P_{Set}	Active power setpoint, in pu
$P_{(V)SM}$	The total real transient power output (pu) of the device, from (3-11), (3-12) or (3-26) as appropriate.
$P(s)$	Governor and prime mover response
ϕ_G	Electrical angle (radians) at distant (stiff) grid
ϕ_R	Electrical angle (radians) of the (virtual) rotor in a (V)SM
ϕ_S	Electrical angle (radians) of the (virtual) stator terminals in a (V)SM
s	Laplace operator $s = j\omega$
ω_0	Nominal system frequency (radians/second)
X	The primary reactance of the SM or VSM device, in pu. For a real SM, this is X'_d , the transient reactance. For a converter, this is normally considered to be the impedance of the primary filter inductor. This can be thought of as the reactance between the (virtual) rotor and (virtual) stator in a (virtual) synchronous machine.
X_G	The additional reactance, in pu, between the (virtual) stator and a convenient grid "point of common coupling" (e.g. a point on the HV grid) that is considered to be a stiff source
ζ	Damping ratio of the SM or VSM rotor dynamics. $\zeta = 1$ corresponds to critical damping.

Table 3-1 Nomenclature for Figure 3-1

From Figure 3-1 the response of the (virtual) rotor can be deduced:

$$\frac{\phi_R}{\phi_G} = \frac{\left(\frac{\omega_0}{s}\right)\left(\frac{X}{(X+X_G)}\right)F_\delta(s)F_R(s)\left\{\frac{1}{X} + F_S(s)\frac{k_S \cdot s}{\omega_0}\right\}}{\left(2Hs + \left[\left(\frac{\omega_0}{s}\right)\left(\frac{X}{(X+X_G)}\right)F_\delta(s)F_R(s)\left\{\frac{1}{X} + F_S(s)\frac{k_S \cdot s}{\omega_0}\right\}\right] + \frac{P(s)F_R(s)}{D_f}\right)} \quad (3-1)$$

In its full form this is difficult to analyse or understand. However, if the simplifications are made that $F_\delta(s) \approx 1$, $F_R(s) \approx 1$ and $F_S(s) \approx 1$ (both reasonably approximate for analysis $\ll 50$ Hz), and in the absence of a prime mover response ($D_f \rightarrow \infty$), then (3-1) reduces to:

$$\frac{\phi_R}{\phi_G} \approx \frac{\left(\frac{k_S X}{2H(X+X_G)}s\right) + \left(\frac{\omega_0}{2H(X+X_G)}\right)}{\left(s^2 + \frac{k_S X}{2H(X+X_G)}s + \frac{\omega_0}{2H(X+X_G)}\right)} \quad (3-2)$$

This represents a 2nd-order bandpass filter plus a 2nd-order lowpass filter.

The denominator of these terms reveals a lot about the 2nd order transfer function behaviour [The full time-domain response, equivalent to (3-2) is derived in [3] (Appendix A) for reference].

$$s^2 + \frac{k_s X}{2H(X + X_G)} s + \frac{\omega_0}{2H(X + X_G)} \Leftrightarrow s^2 + 2\zeta\omega_n s + \omega_n^2 \quad (3-3)$$

Where ζ is the damping ratio ($\zeta = 1$ corresponds to critical damping), and ω_n is the undamped resonant frequency in rads/s. Therefore the device will respond to phase steps on ϕ_G with decaying sinusoidal ϕ_R with:

$$\text{undamped resonance at } \omega_n = \sqrt{\frac{\omega_0}{2H(X + X_G)}} \quad (3-4)$$

$$\text{damping ratio } \zeta = \frac{k_s X}{4H\omega_n(X + X_G)} \quad (3-5)$$

$$\text{damped natural resonance at } \omega_d = \omega_n \sqrt{(1 - \zeta^2)} \quad (3-6)$$

(3-4) and (3-5) can also be re-manipulated to reveal the following relationships, any of which can be used when they are convenient or useful:

$$k_s = \frac{4\zeta H\omega_n(X + X_G)}{X} \quad (\text{inverse of (3-5)}) \quad (3-7)$$

$$\zeta = \frac{k_s X}{2\sqrt{2H\omega_0(X + X_G)}} \quad (3-4) \text{ \& (3-5)} \quad (3-8)$$

$$k_s = \frac{2\zeta\sqrt{2H\omega_0(X + X_G)}}{X} \quad (\text{inverse of (3-8)}) \quad (3-9)$$

Equation (3-1) for a (V)SM is an important stage in determining the output power response to be determined, for a grid frequency disturbance f_g that causes a phase disturbance ϕ_G (Figure 3-1). This will be the Network Frequency Perturbation plot [3].

3.2 Simple Generic(V)SM model example : Network Frequency Perturbation (NFP) plot

The NFP plot [2][3] relates a grid frequency/phase perturbation to an active power response at the device terminals. There are 3 other plots in the family of responses (see section 1.1, and [3]), but the NFP plot is the most important.

From Figure 3-1, for a real SM or VSM_{Ext}:

$$R_{NFP} = \left(\frac{P_{SM} \text{ or } P_{VSM_{Ext}}}{f_g} \right) = \frac{\left(\frac{X}{(X + X_G)} \right) F_\delta(s) \left\{ \frac{1}{X} + F_s(s) \frac{k_s \cdot s}{\omega_0} \right\} (\phi_R - \phi_G)}{\left(\frac{\phi_G}{\left(\frac{\omega_0}{s} \right)} \right)} \quad (3-10)$$

which manipulates to (for a real SM or VSM_{Ext}):

$$R_{NFP} = \left(\frac{P_{SM} \text{ or } P_{VSM_{Ext}}}{f_g} \right) = \left(\frac{\omega_0}{s} \right) \left(\frac{X}{(X + X_G)} \right) F_\delta(s) \left\{ \frac{1}{X} + F_s(s) \frac{k_s \cdot s}{\omega_0} \right\} \left(\frac{\phi_R}{\phi_G} - 1 \right) \quad (3-11)$$

and similarly, from Figure 3-1, for a VSM_{Int}:

$$R_{NFP} = \left(\frac{P_{VSM_{Int}}}{f_g} \right) = \left(\frac{\omega_0}{s} \right) \left(\frac{X}{(X + X_G)} \right) F_\delta(s) \left\{ \frac{1}{X} \right\} \left(\frac{\phi_R}{\phi_G} - 1 \right) \quad (3-12)$$

In both (3-11) & (3-12), the value ϕ_R/ϕ_G is obtained via (3-1). Equations (3-11) & (3-12) can be used to evaluate the Network Frequency Perturbation (NFP) plot for a SM or VSM_{Ext}, or a VSM_{Int}. These equations define the active-power responses of simple (V)SM devices to changes in grid frequency and phase. These equations are used to generate the actual response curve shown in Figure 2-2 and Figure 2-3.

It is clear that the NFP plot for a device is dependent on, not only the device parameters, but ALSO the upstream grid impedance X_G . This means that the NFP plot for an individual unit in a power park varies with:

- upstream impedance as it actually exists in Ohms (overhead lines, cables, transformers), in per unit on the basis of the park rating

- number of turbines operating in a power park, in a common-mode fashion. If only some of the units within a power park are operating, then the effective rating of the power park is lower, and the upstream impedance X_G , as a per-unit value, is decreased.

3.2.1 Simple Generic(V)SM model example : Network Frequency Perturbation (NFP) plot : point of maximum amplitude

(3-12) can be expanded as follows:

$$\left(\frac{P_{VSMInt}}{f_g}\right) = \left(\frac{\omega_0}{s}\right) \left(\frac{X}{(X + X_G)}\right) F_\delta(s) \left\{\frac{1}{X}\right\} \left(\frac{\left(\frac{\omega_0}{s}\right) \left(\frac{X}{(X + X_G)}\right) F_\delta(s) F_R(s) \left\{\frac{1}{X} + F_S(s) \frac{k_S \cdot s}{\omega_0}\right\}}{\left(2Hs + \left[\left(\frac{\omega_0}{s}\right) \left(\frac{X}{(X + X_G)}\right) F_\delta(s) F_R(s) \left\{\frac{1}{X} + F_S(s) \frac{k_S \cdot s}{\omega_0}\right\}\right] + \frac{P(s)F_R(s)}{D_f}\right)} - 1 \right) \quad (3-13)$$

$$\left(\frac{P_{VSMInt}}{f_g}\right) = \left(\frac{\omega_0}{s}\right) \left(\frac{X}{(X + X_G)}\right) F_\delta(s) \left\{\frac{1}{X}\right\} \left(\frac{\left(\frac{\omega_0}{s}\right) \left(\frac{X}{(X + X_G)}\right) F_\delta(s) F_R(s) \left\{\frac{1}{X} + F_S(s) \frac{k_S \cdot s}{\omega_0}\right\} - \left(2Hs + \left[\left(\frac{\omega_0}{s}\right) \left(\frac{X}{(X + X_G)}\right) F_\delta(s) F_R(s) \left\{\frac{1}{X} + F_S(s) \frac{k_S \cdot s}{\omega_0}\right\}\right] + \frac{P(s)F_R(s)}{D_f}\right)}{\left(2Hs + \left[\left(\frac{\omega_0}{s}\right) \left(\frac{X}{(X + X_G)}\right) F_\delta(s) F_R(s) \left\{\frac{1}{X} + F_S(s) \frac{k_S \cdot s}{\omega_0}\right\}\right] + \frac{P(s)F_R(s)}{D_f}\right)} \right) \quad (3-14)$$

$$\left(\frac{P_{VSMInt}}{f_g}\right) = \left(\frac{\omega_0}{s}\right) \left(\frac{X}{(X + X_G)}\right) F_\delta(s) \left\{\frac{1}{X}\right\} \left(\frac{-\left(2Hs - \frac{P(s)F_R(s)}{D_f}\right)}{\left(2Hs + \left[\left(\frac{\omega_0}{s}\right) \left(\frac{X}{(X + X_G)}\right) F_\delta(s) F_R(s) \left\{\frac{1}{X} + F_S(s) \frac{k_S \cdot s}{\omega_0}\right\}\right] + \frac{P(s)F_R(s)}{D_f}\right)} \right) \quad (3-15)$$

if the simplifications are made that $F_\delta(s) \approx 1$, $F_R(s) \approx 1$ and $F_S(s) \approx 1$ (both reasonably approximate for analysis $\ll 50$ Hz), and in the absence of a prime mover response ($D_f \rightarrow \infty$), then (3-15) reduces to:

$$\left(\frac{P_{VSMInt}}{f_g}\right) \approx \left(\frac{\omega_0}{s}\right) \left(\frac{1}{(X + X_G)}\right) \left(\frac{-2Hs}{\left(2Hs + \left[\left(\frac{\omega_0}{s}\right) \left(\frac{X}{(X + X_G)}\right) \left\{\frac{1}{X} + \frac{k_S \cdot s}{\omega_0}\right\}\right]\right)} \right) \quad (3-16)$$

$$\left(\frac{P_{VSMInt}}{f_g}\right) \approx \left(\frac{\omega_0}{(X + X_G)}\right) \left(\frac{-2Hs}{\left(2Hs^2 + \left[\omega_0 \left(\frac{X}{(X + X_G)}\right) \left\{\frac{1}{X} + \frac{k_S \cdot s}{\omega_0}\right\}\right]\right)} \right) \quad (3-17)$$

$$\left(\frac{P_{VSMInt}}{f_g}\right) \approx -\left(\frac{\omega_0}{(X + X_G)}\right) \left(\frac{s}{\left(s^2 + \left(\frac{k_S}{2H}\right) \left(\frac{X}{(X + X_G)}\right) s + \left(\frac{\omega_0}{2H}\right) \left(\frac{1}{(X + X_G)}\right)\right)} \right) \quad (3-18)$$

This will have maximum amplitude when (roughly) the s^2 term cancels with the $\left(\frac{\omega_0}{2H}\right)\left(\frac{1}{(X+X_G)}\right)$ term at a frequency of ω_n as given by (3-4).

The maximum amplitude will be roughly:

$$|R_{NFP_max}| \approx \left| \left(\frac{P_{VSM_Int}}{f_g} \right)_{max} \right| \approx \left(\frac{\omega_0}{(X+X_G)} \right) \left(\frac{s}{\left(\left(\frac{k_s}{2H} \right) \left(\frac{X}{(X+X_G)} \right) s \right)} \right) \approx \omega_0 \left(\frac{2H}{k_s X} \right) \quad (3-19)$$

A final step using (3-9) relates this to the damping coefficient zeta ζ :

The maximum amplitude will be roughly:

$$|R_{NFP_max}| \approx \left| \left(\frac{P_{VSM_Int}}{f_g} \right)_{max} \right| \approx \omega_0 \left(\frac{2H}{k_s X} \right) \approx \omega_0 \left(\frac{2H}{\left(\frac{2\zeta \sqrt{2H\omega_0(X+X_G)}}{X} \right) X} \right) \quad (3-20)$$

$$|R_{NFP_max}| \approx \left| \left(\frac{P_{VSM_Int}}{f_g} \right)_{max} \right| \approx \frac{1}{\zeta} \sqrt{\frac{\omega_0 H}{2(X+X_G)}} \quad (3-21)$$

This final answer (3-21) for the (approximate) peak response can become very useful in interpreting the NFP plot and understanding how the damping coefficient shapes the response, relative to the intercept of the asymptotes, and where the inertia asymptote crosses the natural frequency ω_n

3.2.2 Simple Generic(V)SM model example : Network Frequency Perturbation (NFP) plot : estimation of damping coefficient zeta ζ from the NFP plot

There is another very useful relationship which can be determined from the NFP amplitude plot and its position relative to the crossing of the inertia and undamped phase step asymptotes. This can be applied after estimating H and $(X+X_G)$ as described in sections 0 and 0.

The NFP response for a VSM is given in (3-15). This was expanded and analysed, leading to an expression (3-21) for the approximate peak amplitude of the NFP plot, accounting for damping.

Now this can be compared to the amplitude at which the inertia and zero-damping phase-step asymptotes intersect, given by (2-16). Combining (2-16) and (3-21) leads to:

$$\frac{|R_{NFP_InertiaAsymptoteAtUndampedResonanceFrequency}|}{|R_{NFP_max}|} \approx \frac{\sqrt{\frac{2H\omega_0}{(X+X_G)}}}{\frac{1}{\zeta} \sqrt{\frac{\omega_0 H}{2(X+X_G)}}} \quad (3-22)$$

Finally this extremely helpful equation drops out:

$$\zeta \approx \frac{|R_{NFP_InertiaAsymptoteAtUndampedResonanceFrequency}|}{2|R_{NFP_max}|} \quad (3-23)$$

This means that the damping coefficient zeta, ζ is related very simply to the ratio between the peak NFP amplitude response and the amplitude at the point at which the inertia and the zero-damping phase-step asymptotes cross. The peak NFP amplitude response and the asymptote crossing should both occur roughly at the undamped resonant frequency at $2\pi f_{NFP_mod} = \omega_n = 2\pi \cdot f_n$. If the zero-damping phase-step asymptote is not available or is unclear, then the inertia asymptote line can be used alone, with its amplitude sampled at the undamped resonant frequency.

3.3 Simple Generic(V)SM model example : Power output response to a reference command change

While not important for the NFP plot generation, it is useful to also note the following relationship. For the generic VSM of (Figure 3-1), the output power response to a change in reference input power P_{Set} can be written as:

$$f_R = \frac{F_R(s)}{2Hs} \left[P(s) \left(P_{Set} - \frac{f_R}{D_f} \right) - \left(\frac{\omega_0}{s} \right) \left(\frac{X}{(X + X_G)} \right) F_\delta(s) \left\{ \frac{1}{X} + F_S(s) \frac{k_S \cdot s}{\omega_0} \right\} f_R \right] \quad (3-24)$$

which evaluates as a relationship between f_R and P_{Set} :

$$\frac{f_R}{P_{Set}} = \frac{F_R(s)P(s)}{\left(2Hs + \left(\frac{\omega_0}{s} \right) \left(\frac{X}{(X + X_G)} \right) F_\delta(s)F_R(s) \left\{ \frac{1}{X} + F_S(s) \frac{k_S \cdot s}{\omega_0} \right\} + \frac{F_R(s)P(s)}{D_f} \right)} \quad (3-25)$$

This can be taken on to the expression for P_{VSMInt} in response to P_{Set} :

$$\frac{P_{VSMInt}}{P_{Set}} = \left(\frac{\omega_0}{s} \right) \left(\frac{X}{(X + X_G)} \right) F_\delta(s) \left\{ \frac{1}{X} \right\} \left(\frac{f_R}{P_{Set}} \right) \quad (3-26)$$

4 Practical considerations

4.1 Practical considerations : time domain considerations and test waveforms

During the NFP sweep, the grid voltage frequency $f(t)$ is defined by (2-1), which defines a sinusoidal frequency modulation on the applied V_{abc} grid voltages at the distant “infinite bus”. It can also be thought of as a phase modulation, since frequency modulation and phase modulation are equivalent if the modulating signal is sinusoidal. For example:

$$\Phi(t) = \int 2\pi f(t) \cdot dt = \int 2\pi (f_0 + \Delta f \cos(2\pi f_{NFP_{mod}} t + \phi_{\Delta f})) \cdot dt \quad (4-1)$$

$$\Phi(t) = 2\pi f_0 t + \frac{2\pi \Delta f}{2\pi f_{NFP_{mod}}} \sin(2\pi f_{NFP_{mod}} t + \phi_{\Delta f}) + c \quad (\text{Assuming } f_{NFP_{mod}} \text{ is constant}) \quad (4-2)$$

So, for example, in a time-domain environment when $f_{NFP_{mod}}$ is held constant, the applied grid voltages could be generated by an expression such as:

$$V_{abc}(t) = V \cos \left(2\pi f_0 t + \frac{2\pi \Delta f}{2\pi f_{NFP_{mod}}} \sin(2\pi f_{NFP_{mod}} t + \phi_{\Delta f}) + \begin{bmatrix} 0 \\ -2\pi/3 \\ 2\pi/3 \end{bmatrix} \right) \quad (4-3)$$

However in practice, if it is desired to sweep the NFP frequency $f_{NFP_{mod}}$ across a number of values in a single simulation, such that $f_{NFP_{mod}}$ is not constant against t , but only piecewise-constant, then the final equations are more complex than (2-1) and (4-1)-(4-3). In this case it is more practical in the simulation environment to create $f(t)$ from a rolling real-time integration of $f_{NFP_{mod}}$ (which can be varied or stepped in real time). Then phase $\Phi(t)$ can similarly be created with a dynamic numerical integrator from $f(t)$ and finally $V_{abc}(t)$ dynamically created from $\Phi(t)$.

4.1.1 Practical considerations : frequency spectra of grid voltages during an NFP plot

During a time period where $f_{NFP_{mod}}$ is held constant, the grid voltages are frequency/phase modulated signals, where the modulation is sinusoidal FM/PM, onto a sinusoidal carrier at f_0 . The frequency spectra of the grid voltages $V_{abc}(t)$, thus modulated, are described by a Bessel function of the first kind. The modulation index for a generic sinusoidally-modulated FM signal is defined by

$$h = \frac{\Delta f}{f_m} \text{ in the context of a signal defined by } y(t) = A \cos \left(2\pi f_c t + \frac{\Delta f}{f_m} \sin(2\pi f_m t) \right) \quad (4-4)$$

By comparing the form and details of this generic FM definition with (4-3), it can be determined that during the NFP plot the modulation index h is:

$$h = \frac{\Delta f}{f_m} = \frac{\Delta f}{f_{NFP_{mod}}} \quad (4-5)$$

During the NFP plot, the maximum frequency deviation Δf is limited by the equations in (2-3).

At low $f_{NFP_{mod}}$ with $f_{NFP_{mod}}$ down to 0.001 Hz for example, these allow $\Delta f \gg f_{NFP_{mod}}$ and therefore modulation index $h \gg 1$, in which case there are multiple FM sidebands in the spectra, it is considered to be “wideband FM” and the FM bandwidth can be considered to be $\sim 2\Delta f$. At high $f_{NFP_{mod}}$, (2-3) restricts Δf to:

$$\Delta f < \frac{\Delta P_{max}}{2H} \frac{f_0}{2\pi f_{NFP_{mod}}} \quad (4-6)$$

and therefore:

$$h < \frac{\left(\frac{\Delta P_{max}}{2H} \frac{f_0}{2\pi f_{NFP_{mod}}} \right)}{f_{NFP_{mod}}} \quad (4-7)$$

$$h < \frac{\Delta P_{max}}{4\pi H} \frac{f_0}{f_{NFP_{mod}}^2} \quad (4-8)$$

Since a sensible upper limit of exploration of $f_{NFP_{mod}}$ is f_0 , this puts an upper bound on h , at the upper values of $f_{NFP_{mod}}$, at:

$$h < \frac{\Delta P_{max}}{4\pi H} \quad (4-9)$$

Depending on ΔP_{max} allowed during the NFP test (see (3-27)), and the setting of inertia H , this can allow values of h less than unity. If $h \ll 1$, then the FM is considered to be “narrowband FM” and the bandwidth can be considered to be $\sim 2f_{NFP_{mod}}$.

For intermediate values of h , it can be seen that the bandwidth of the FM spectra signal could be considered to be roughly the maximum of the two values: $2\Delta f$ or $2f_{NFP_{mod}}$.

4.2 Practical considerations : carrying out response sweeps for NFP and NVP plots in simulation and real-world environments

Within time-domain simulations and when real-world device implementations are involved, evaluation of the device responses to the modulated frequency/phase or voltage magnitudes need careful consideration. Here it is useful to recall that there are 4 possible plots in the NFP family (see section 1.1). The “NFP” pair of plots require a sinusoidal modulation of the frequency/phase of the voltage waveforms, while the “NVP” pair of plots require a sinusoidal modulation of voltage amplitude.

Due to the assumed reciprocity of the total grid impedance, between the distant upstream “infinite bus” and the (virtual) device rotor (Figure 2-1), it is possible to either:

- modulate the frequency/phase/voltage of either the distant upstream grid voltages
- OR to instead artificially place the modulation at the (virtual) rotor.

In theory, both will draw out the same active and reactive power flows, if the modulated deviations are applied oppositely at the (virtual) rotor to they were at the grid, or if the resulting P/Q values are negated.

When the distant upstream grid voltages are modulated, then this requires either

- the entire analysis to be done in simulation
- OR, a CHIL environment can be used to directly test the device (controller) response
- OR, a PHIL environment can be used to directly test the whole device response (including power hardware). In this case, the PHIL environment needs to be rated appropriately for the device. This requirement may preclude such PHIL testing for MW and multi-MW scale devices.

The alternative, which is available for VSM devices, is to instead make a direct modulation of the voltages applied to the converter bridge virtual rotor, E_{abc} , Figure 2-1, using direct signal injection. For the test to have a meaningful result:

- For NFP sweeps (see section 1.1), the frequency/phase modulation must be applied by injecting the required signal at f_R (frequency modulation) or ϕ_R (phase modulation). The injected signals must not be routed anywhere within the device’s control system, apart from via the direct path to the modulated waveforms E_{abc} . This means that if the signals f_R or ϕ_R are part of feedback loops within the software, then the signal injection must be placed AFTER the fed-back signals are generated, but before the final PWM modulator.
- For NVP sweeps (see section 1.1), the amplitude modulation must be applied by injecting the required signal at the point where the PWM modulator actually sets the virtual rotor modulation depth. The injected signals must not be routed anywhere within the device’s control system, apart from via the direct path to the modulated waveforms E_{abc} . The signal injection must be placed AFTER any fed-back signals are generated, but before the final PWM modulator.
- Either the modulations need to be inverted, or the measured P/Q values negated, compared to the “normal” test configuration, when the grid voltages are manipulated.
- When using this method, consideration has to be made about the **effective** grid stiffness. For example, if a power park contains many individual GF power units, then the Short Circuit Ratio (SCR) and grid impedance X_G (see section 3.2) are usually assessed on the basis that all units operated in an aggregated, common-mode, fashion. However, if the individual power units within that park operate with different modulating power/phase/voltage profiles, then the **effective** grid stiffness, as “perceived” by each individual power unit, can be much stiffer than the quoted park SCR suggests, in terms of the reaction at that modulation

frequency. This is because the operation of the individual units become decorrelated, and there are increased differential-mode but decreased common-mode actions. In particular, if an NFP sweep is done, using internal signal injection, using just a single unit within a large power park, then the grid will appear very stiff to that particular unit, at each modulation frequency used. This is especially true if the units are all GF units, as each other GF unit will tend to make the local grid stiffer, unless it ALSO has the same modulated NFP injections made. It will not be possible to create the NFP plot for the whole park operating in an aggregated fashion, without either:

- injecting the same NFP modulation signals to the bridges, in a time-synchronised manner, to all power units, simultaneously.
- OR, inserting an additional impedance upstream of a single unit, so that the per-unit impedance value of that additional impedance (on the rating of that single unit) matches the per-unit value of the normal park upstream impedance, on the rating of the whole park.
- OR, accepting that the above two options are not trivial, and this may mean that practical on-site testing of such units within power parks only feasibly represents stiff grid scenarios, and that to investigate weak-grid common-mode reactions to NFP stimuli at the grid side, practically requires simulation rather than on-site testing.

4.2.1 Practical considerations : NFP sweeps in practice

The following are guidelines or items to consider when carrying out an NFP type plot.

The value of $f_{NFP_{mod}}$ is swept across a broad range, from (ideally) 0.001 Hz to 50 Hz, while $\phi_{\Delta f}$ should generally be kept constant. In practice a range of **0.02 Hz** $< f_{NFP_{mod}} < 50$ Hz is more appropriate, due to the excessively long periods of $f_{NFP_{mod}}$ at frequencies below 0.02 Hz.

The saturation limits listed in (2-3) must be considered.

It is important that the acquisition system be able to sample the disturbance signal $f(t)$ (2-1) coherently with the signal $P_{out}(t)$ (2-2), without filtering effects or unequal time latency/lag in either acquisition channel that skew or colour the data.

It is also important that the duration of the signal generation and signal acquisition, for each value of $f_{NFP_{mod}}$, is long enough to capture at least 2 or more periods of $f_{NFP_{mod}}$, preferable 5 or more. Where $f_{NFP_{mod}}$ is small and the period becomes large so that only a few periods can be captured, it becomes important also to ensure that the data capture length is an integer multiple of the $f_{NFP_{mod}}$ period, to reduce spectral leakage in the subsequent DFT operations.

As a target the channels must be aligned within:

$$\Delta t < \frac{2}{360 \cdot f_{NFP_{mod}}} \text{ seconds} \quad (4-10)$$

to achieve a phase accuracy of 2 degrees. For example this is approx 100 μ s (equivalent to 1 sample at 10 kHz), to give a ~2 degree accuracy in NFP phase response accuracy at 50 Hz. Larger errors are tolerable at lower values of $f_{NFP_{mod}}$, and is useful for those low values of $f_{NFP_{mod}}$ where acquisition times need to be extended. This means that as acquisition times are extended, the sample rates can be reduced and the coherence tolerance increases by (4-10).

So (as an example):

- 1) Calculate the integer number of periods which are required to fill 5 seconds

$$\circ N_5 = \text{ceil}(5f_{NFP_{mod}})$$

- 2) If $N_5 > 2$ then set $t_{Acquisition} = \frac{N_5}{f_{NFP_{mod}}}$

- 3) Otherwise, set $t_{Acquisition} = \frac{2}{f_{NFP_{mod}}}$

- 4) Configure the signal generation and acquisition (plot) devices to $t_{Acquisition}$ so that an integer number of periods of $f_{NFP_{mod}}$ are captured.

The acquisition system must, for each frequency point $f_{NFP_{mod}}$,

- Generate the frequency disturbance by (2-1) and/or the principles outlined in section 4.1
- Apply the signal and allow a suitable settling period, e.g. 10 seconds or $t_{Acquisition}$, whichever is the shorter.
- Capture the time-domain samples of $f(t)$ and $P_{out}(t)$ for a period of at least $t_{Acquisition}$, and then (rectangular) window them to $t_{Acquisition}$ seconds if necessary.
 - Note, in this context, P_{out} should not contain any filtering and should be taken directly from P_{inst} , the instantaneous active power.
- remove DC bias
- perform DFTs on the AC residues, using suitable (e.g. Hanning) windows (length $t_{Acquisition}$) revealing
 - $\Delta f \angle \phi_{\Delta f}$, the input frequency disturbance, extracted from the DFT of P_{out} at the spot frequency $f_{NFP_{mod}}$
 - $\Delta P \angle \phi_{\Delta P}$, the output power response component, extracted from the DFT of P_{out} at the spot frequency $f_{NFP_{mod}}$
 - The required spot frequency may not correspond exactly to a DFT “bin”, so in this case a suitable interpolation algorithm should be used over the nearest DFT “bin” frequency points.
- calculate the response R_{NFP} :

$$R_{NFP} = |R_{NFP}| \angle R_{NFP} = \frac{\Delta P \angle \phi_{\Delta P}}{\left(\frac{\Delta f \angle \phi_{\Delta f}}{f_0} \right)} \quad (4-11)$$

4.2.1.1 The NFPxQ plot

The NFPxQ plot (see section 1.1) can be gathered in exactly the same way as the NFP plot, using the same stimulus waveform, applied to either grid frequency/phase, or injected via virtual rotor frequency/phase. However, the measured power will be Q_{out} , reactive power, instead of P_{out} , active power.

In this context, Q_{out} should ideally not contain any filtering and therefore should perhaps be taken from Q_{inst} , an “instantaneous” reactive power. However, an unfiltered Q_{out} measurand has debateable physical significance, and it may make more sense to accept a Q_{out} perception over (for example) single-cycle periods, and limit the upper frequency shown on the NVP plot to (for example) half the fundamental frequency.

The NFPxQ response will be :

$$R_{NFPxQ} = |R_{NFPxQ}| \angle R_{NFPxQ} = \frac{\Delta Q \angle \phi_{\Delta Q}}{\left(\frac{\Delta f \angle \phi_{\Delta f}}{f_0} \right)} \quad (4-12)$$

4.2.2 Practical considerations : NVP sweeps in practice

To create the stimulus, the grid (or virtual rotor) voltage magnitude should be modulated:

$$|V| = 1 + V_{Dist} \quad (\text{in pu}) \quad (4-13)$$

where

$$V_{Dist} = \Delta V \cos(2\pi f_{NVP_{mod}} t + \phi_{\Delta V}) \quad (4-14)$$

$f_{NVP_{mod}}$ should be swept as for the NFP plot.

The magnitude of ΔV should be selected for each $f_{NVP_{mod}}$ point, so that dV_{Dist}/dt does not exceed 1.0 pu/s (this is a somewhat arbitrary value chosen by the author at the time of writing, based solely on engineering judgement). The magnitude of ΔV should also be small enough that it cannot push the device into current limit, accounting for aggressive droop slopes that may be in place.

This means that (as an example guide):

$$\Delta V < \frac{1.0}{2\pi f_{NVP_{mod}}} \text{ pu} \quad (\text{whichever is smaller}). \quad (4-15)$$

$$\Delta V < 0.05 \text{ pu}$$

The same considerations about signal injection and data acquisition should be applied, as described for the NFP plots in sections 4.2 and 4.2.1.

4.2.2.1 The NVP plot

The NVP response assesses the reactive power modulation at frequency $f_{NVP_{mod}}$, the the voltage change:

$$R_{NVP} = |R_{NVP}| \angle R_{NVP} = \frac{\Delta Q \angle \phi_{\Delta Q}}{\Delta V \angle \phi_{\Delta V}} \quad (4-16)$$

In this context, Q_{out} should ideally not contain any filtering and therefore should perhaps be taken from Q_{inst} , an “instantaneous” reactive power. However, an unfiltered Q_{out} measurand has debateable physical significance, and it may make more sense to accept a Q_{out} perception over (for example) single-cycle periods, and limit the upper frequency shown on the NVP plot to (for example) half the fundamental frequency.

4.2.2.2 The NVPxP plot

The cross-product response from voltage disturbance to active power response can be gathered and plotted in exactly the same way as the NVP plot, as described in sections 4.2.2 and 4.2.2.1, **except** that the measured power will be P_{out} , active power, instead of Q_{out} , reactive power.

In this context, P_{out} should not contain any filtering and therefore should be taken directly from P_{inst} , the instantaneous active power.

The NVPxP response will be :

$$R_{NVPxP} = |R_{NVPxP}| \angle R_{NVPxP} = \frac{\Delta P \angle \phi_{\Delta P}}{\Delta V \angle \phi_{\Delta V}} \quad (4-17)$$

5 Reverse engineering an NFP plot to determine (V)SM parameters

5.1 Deducing VSM parameters H , ζ , etc. from the NFP plot

Given an NFP plot, it is possible to determine the parameters for a generic VSM model (Figure 3-1) from the NFP plot (e.g. Figure 2-2 & Figure 2-3), with good accuracy, if the NFP plot belongs to a device that is a good match for the generic VSM model (Figure 3-1), placed within a grid, test, or simulation scenario which is also a good match for the generic VSM model (Figure 3-1).

There are several procedures of varying complexity which allow reverse-engineering of the generic VSM model parameters from the NFP plot. The below sections give examples, but there will be other ways and methods to be discovered.

5.1.1 Basic estimation of droop response from the NFP plot

The droop response (if present) can be estimated from the reciprocal of the magnitude of the NFP plot as modulation frequency approaches zero. The NFP plot phase should approach 180° in this case, at that part of the NFP plot.

5.1.2 Basic estimation of H from the NFP plot inertia asymptote

The most basic reverse-engineering of H is to estimate H from the part of the NFP plot that approaches the inertia asymptote (see section 2.4.2). The hard part is:

- To pick the correct frequency range of the NFP plot, which might (roughly) match the inertia asymptote.
- Even the ideal generic VSM NFP plot does not exactly overlay the inertia asymptote, so the fit can only ever be approximate with this simple analysis

Nevertheless, a relatively basic curve-fitting technique and gradient estimation, over a restricted frequency range, can yield reasonable results, as shown by the example of the thin yellow dotted line, deduced in Figure 2-2. This estimates an inertia $H=4.41$ s, against an actual value of $H=4.0$ s, in the example shown.

5.1.3 Basic estimation of total bridge-grid impedance ($X + X_G$)

It is also possible to estimate $(X + X_G)$ from the NFP plot by fitting a “downslope” to the NFP plot, over the upper part of the frequency range from the peak of the NFP plot (amplitudes) to the highest frequency point on the NFP plot. This is where the phase-step response asymptote (see section 2.4.3) is dominant.

The key equation is (2-12) which gives:

$$R_{NFP} \approx j \left(\frac{f_0}{f_{NFP_{mod}}} \right) \left(\frac{1}{(X + X_G)} \right) \quad (5-1)$$

Because this expression is proportional to the reciprocal of $f_{NFP_{mod}}$, the easiest curve fit is obtained by fitting to the reciprocal of $|R_{NFP}|$.

This means that:

$$\frac{1}{|R_{NFP}|} \approx f_{NFP_{mod}} \left(\frac{(X + X_G)}{f_0} \right) \quad (5-2)$$

$$\frac{d \left(\frac{1}{|R_{NFP}|} \right)}{df} \approx \left(\frac{(X + X_G)}{f_0} \right) \quad (5-3)$$

The hard part of this is:

- To pick the correct frequency range of the NFP plot, which might (roughly) match the phase-step asymptote.
- Even the ideal generic VSM NFP plot does not exactly overlay the phase-step asymptote, so the fit can only ever be approximate with this simple analysis

On the example Figure 2-2, this procedure led to an estimated $(X + X_G)$ of 0.30 pu, against an actual modelled value of 0.29 pu. By combining this value with the estimated inertia $H=4.41$ s, the undamped natural frequency was also estimated on Figure 2-2, using (2-14), at $f_n=1.73$ Hz, against an actual modelled value of 1.85 Hz.

5.1.4 Basic estimation of ζ : How to determine $|R_{NFP_max}|$ and $\omega_n = 2\pi \cdot f_n$

The tricky part is how to determine $|R_{NFP_max}|$ and $\omega_n = 2\pi \cdot f_n$ from the NFP plot.

A first guess would be literally to extract the maximum response $|R_{NFP_max}|$ and assign $\omega_n = 2\pi \cdot f_n$ to be the frequency at which that appears on this plot. However, if this approach is taken, it is relatively inaccurate. The yellow asterisk markers on Figure 2-2 show how using this method could work

To estimate the damping this way you still also need to guess at the inertia H or estimate it using section 5.1.2. In the example shown, even with a perfectly guessed H , the estimated f_n and ζ values are in error by 35-40 %

Of course if you already know H , $(X + X_G)$, and therefore $\omega_n = 2\pi \cdot f_n$ by (3-4), then you can place different markers on the example Figure 2-2, i.e. the yellow '+' markers at the exactly correct f_n . (On Figure 2-2 they are mostly obscured behind the circle markers). This leads to an exact determination of the correct ζ value, which is more a test of the equation (3-23) than anything else.

What is more useful is to follow the procedures in sections 5.1.2 and 5.1.3 to estimate H , $(X + X_G)$, and therefore $\omega_n = 2\pi \cdot f_n$ by (3-4), all done from the NFP plot itself. This gives a reasonable estimate, without cheating, of f_n and allows equation (3-23) to be evaluated with the estimated values. The example markers on Figure 2-2 are the yellow circles

This procedure can ultimately lead to quite accurate results. In the example of Figure 2-2:

- H estimates as 4.40 (actual was 4.00)
- $(X + X_G)$ estimates as 0.30 (actual was 0.29)
- f_n estimates as 1.73 (actual was 1.85)
- ζ estimates as 1.07 (actual was 1.00)

5.1.5 Estimation of all parameters from NFP plot using multi-parameter fit

As an alternative, or as a follow-on to the estimation procedures described in sections 5.1.1 to 5.1.4, a more complex fitting process can be carried out. This could be achieved using one of a number of "optimisation" techniques that allow minimisation of an error function so that the closest possible match of model parameterised by a number of parameters, to a set of data, can be found.

For example, in the example there are 7 parameters that are fitted to attempt to match the Generic VSM model performance shown in Figure 2-2 & Figure 2-3:

- H
- $(X + X_G)$
- ζ
- τ_s which sets the time constant for $F_s(s)$
- D_f droop slope
- τ_p which sets the time constant for $P(s)$
- τ_δ which sets the time constant for $F_\delta(s)$

These can be initially populated (seeded) with initial guesses, optionally including data obtained from prior basic estimations described in sections 5.1.1 to 5.1.4.

By creating a suitable error function, and operating the optimisation in a suitable manner, it is possible to obtain a very good match to an NFP plot that was created with the Generic VSM model. This is mostly a test of the fitting process since the same model is being used for both NFP plot generation and the fitting process, so the fit can get very close if it works properly.

An example is shown in the "Full parameter fit" trace (black dashed line) on Figure 2-2 & Figure 2-3 which overlies the original data almost exactly, and the deduced parameters are an almost exact match with the original parameters used to generate the data.

When using such a "Full parameter fit", and using the Generic VSM model as a basis, if an NFP plot trace from a device which has a significantly different or more complex control system than the Generic VSM model is input to the fitting process, then the output results may deviate from the published/target/expected values. However, the general assessment of inertia, damping, droop response, etc., should still be correct within some reasonable degree of approximation.

Appendix A Derivation of time-domain response of (V)SM rotor

Equation (3-2) is repeated here as (4), the simplified rotor response, ignoring the additional filters.

$$\frac{\phi_R}{\phi_G} \approx \frac{\frac{k_s X}{2H(X + X_G)}s + \frac{\omega_0}{2H(X + X_G)}}{s^2 + \frac{k_s X}{2H(X + X_G)}s + \frac{\omega_0}{2H(X + X_G)}} \quad (4)$$

This can be rewritten using (3-3) as:

$$\frac{\phi_R}{\phi_G} \approx \frac{2\zeta\omega_n s + \omega_n^2}{s^2 + 2\zeta\omega_n s + \omega_n^2} \quad (5)$$

in which (3-4)-(3-9) can all be applied where useful.

If a phase step function of size Δ radians, i.e. Δ/s is applied at ϕ_G , then the response at ϕ_R will be:

$$\phi_R \approx \frac{\Delta}{s} \left[\frac{2\zeta\omega_n s + \omega_n^2}{s^2 + 2\zeta\omega_n s + \omega_n^2} \right] \quad (6)$$

This can be split into two parts:

$$\phi_R \approx \Delta \left[\frac{2\zeta\omega_n}{s^2 + 2\zeta\omega_n s + \omega_n^2} + \frac{\omega_n^2}{s(s^2 + 2\zeta\omega_n s + \omega_n^2)} \right] \quad (7)$$

A final short set of manipulations allows the two parts to be put into forms that can be applied directly to a table of inverse Laplace transforms:

$$\phi_R \approx \Delta \left[\frac{2\zeta\omega_n}{(s + \zeta\omega_n)^2 - (\zeta\omega_n)^2 + \omega_n^2} + \frac{\omega_n^2}{s(s^2 + 2\zeta\omega_n s + \omega_n^2)} \right] \quad (8)$$

where we can define:

$$\omega_d^2 = \omega_n^2(1 - \zeta^2) \Rightarrow \omega_d = \omega_n\sqrt{1 - \zeta^2} \quad (9)$$

which is essentially where the equation for the damped natural resonance stems from.

therefore:

$$\phi_R \approx \Delta \left[\frac{2\zeta\omega_n}{(s + \zeta\omega_n)^2 - \omega_d^2} + \frac{\omega_n^2}{s(s^2 + 2\zeta\omega_n s + \omega_n^2)} \right] \quad (10)$$

This expression can now be applied to a standard table of inverse Laplace transforms, assuming $\zeta < 1$:

$$\phi_{R(t)} \approx \Delta \left[\left(\frac{2\zeta\omega_n}{\omega_d} \right) e^{(-\zeta\omega_n t)} \sin(\omega_d t) + \left(1 - \frac{e^{(-\zeta\omega_n t)}}{\sqrt{1 - \zeta^2}} \sin(\omega_d t + \arccos(\zeta)) \right) \right] \quad (11)$$